J Mater Sci (2009) 44:1528–1539
DOI 10.1007/s10853-008-3065-4

Volume fraction effect on high strain rate properties of syntactic foam composites

E. Woldesenbet · S. Peter

Received: 27 November 2007 / Accepted: 15 October 2008 / Published online: 6 November 2008

Abstract The volume fraction effect on the high strain rate compressive properties of syntactic foams is characterized using a pulse-shaped Split-Hopkinson Pressure Bar (SHPB) technique. Eighteen different types of syntactic foams are fabricated with the same matrix resin system but six different microballoon volume fractions and three different size microballoons. The volume fractions of the microballoons in the syntactic foams are maintained at 0.1, 0.2, 0.3, 0.4, 0.5, and 0.6. The microballoons have the same mean outer radius of 40 μm, but different internal radii leading to a difference in their density. Analysis is carried out on the effect of microballoon volume fractions on the high strain rate properties for each type of syntactic foam. This approach is helpful in understanding the effect of microballoon reinforcement at different volume fractions on the dynamic compressive properties of syntactic foams. The results at high strain rates are compared to quasi-static strain rate compressive properties of the same material. The results show that there is a decrease in both compressive strength and modulus as the microballoon volume fraction increases for the same type of syntactic foam at all strain rates. However, at strain rates of quasi-static and 450/s, the decrease tends to be gradual across all volume fractions, while for strain rates of 800/s, there is a dramatic decrease from 10 to 20% followed by a gradual decline for most specimens. The fracture mode plays a major role in the dynamic behavior of syntactic foams.

E. Woldesenbet (✉) · S. Peter
Mechanical Engineering Department, Louisiana State University, Baton Rouge, LA 70803, USA
e-mail: woldesen@me.lsu.edu

Introduction

Syntactic foam, a type of closed-cell foam with properties such as high damage tolerance, low density, and high specific strength, has increased use in structural applications in the field of civil, automobile, aeronautical, and marine engineering [1, 2]. Depending on loading and environmental conditions, either open- or close-cell structured foams can be selected for sandwich composites application mainly as core materials [3]. However, close-cell structures give additional advantage of lower moisture absorption coefficient compared to the open-cell structured foams [4]. Syntactic foam core sandwich composites are used as buoyancy aid material in ships and boats. Recently, syntactic foams, which are commonly made of polymeric resin and microballoons, have been widely used in several engineering applications due to their low moisture absorption, good thermal insulation, excellent strength-to-weight ratio, vibration isolation, and low radar cross section properties [5–7].

Syntactic foams provide structural design flexibility as microballoons and matrix can be made up of any material and quantity depending on the desired composite properties. Wall thickness of microballoons, volume fraction of constituents, and interfacial properties can also be accustomed to fabricate syntactic foams exactly as required in a particular application. Large numbers of studies and research activities on the mechanical properties of syntactic foams are mainly focused on the quasi-static properties, such as tension, compression, and flexural properties, and the associated fracture mode behavior [8–15]. However, their dynamic properties are not well understood due to the limited experimental data and the necessary experimental techniques, although many of the foam applications are impact-related.

Several studies are found in the published literature on the high strain rate testing of several types of polymeric foams performed by using various techniques. However, there are only limited studies available on syntactic foams. Drop weight tower [16] or simulated head impact using dynamic impact sled [17] are conducted to characterize the impact energy behavior of a variety of rigid polymers. High strain rate compressive behavior of rigid polyurethane foam with various densities is determined by Chen et al. [18]. They found the peak stress to be strain rate sensitive and expressed it in terms of the square of the foam density. Tensile and compressive properties of polystyrene bead (PSB) foams at various temperatures and strain rates are studied extensively by Rinde et al. [19]. Some of the previous studies on the dynamic properties of honeycomb structures can also be found in the published literature [20, 21]. These studies found an increase of 20–70% in the dynamic crush strength at impact velocities of 30 m/s.

There is however only limited dynamic or high strain rate studies of syntactic foams found in the published literature [22, 23]. Impact fatigue behavior of syntactic foams has been studied with repeated impact of a projectile [24]. Drop weight and air gun ballistic experiments have also been conducted to investigate the strength and expected damage of syntactic foams under impact loading conditions [25, 26]. Aircraft and marine structural applications that use syntactic foams require a fundamental understanding of the foam dynamic mechanical properties because the impact loading conditions may cause unexpected response unlike quasi-static condition. Therefore, syntactic foams should be extensively characterized for high strain rate or dynamic properties using experimental apparatus that would provide stress–strain–strain rate relationships. The data obtained from such an experiment should be used in numerical modeling for more realistic simulations. Additionally, the knowledge gained is critical for the efficient design of syntactic foam structures that could go through impact loading.

The effect of volume fraction on the high strain rate properties of syntactic foams of eighteen different types of syntactic foams is studied in this paper. The high strain rate properties are determined using a split-Hopkinson Pressure Bar (SHPB) apparatus. The syntactic foams are fabricated with the same matrix resin system but six different microballoon volume fractions and three different size microballoons. The volume fractions of the microballoons in the syntactic foams are maintained at 0.1, 0.2, 0.3, 0.4, 0.5, and 0.6. The microballoons have the same mean outer radius of 40 μm, but different internal radii leading to a difference in their density. The specimens are cylindrical in shape with an aspect ratio of 1. The high strain rate test results provide the relationship of dynamic properties of syntactic foams and volume fraction. The effect of volume fraction on the high strain rate values of compressive strength, failure strain, and compressive modulus is observed and analyzed. The high strain rate properties are compared to the results of the quasi-static tests to evaluate the effect of volume fraction at different strain rates. Extensive scanning electron microscopic observations are performed to establish the modes of failure and understand the mechanical properties further.

Experimental procedure

Details of raw materials used for the fabrication of syntactic foam and testing procedures are given below.

Matrix resin

Based on a comparative study of various commercially available epoxy resins, D.E.R. 332, a di-epoxy resin, manufactured by DOW Chemical Company is selected for the study. This resin is called as diglycidyl ether of bisphenol A (DGEBA). The chemical name of this resin is 2,2-bis[4-(2′3′ epoxy propoxy) phenyl] propane. Average epoxide equivalent weight of the epoxy resin is 174.

Diluent

To lower the viscosity of the resin mix a diluent is added. It is difficult to mix large volume of cenospheres in the resin if the viscosity is high. Adding 5% by weight diluent C_{12}–C_{14} aliphatic glycidyl ether, commercially known as ERISYS-8, brings down the viscosity of the resin from about 4,000 cps at 20 °C to about 2,000 cps at the same temperature. The diluent was supplied by CVC Specialty Chemicals. Additional effects of diluent addition are lowering of the modulus of the epoxy with a corresponding increase in ductility. Average equivalent epoxide weight (EEW) of the diluent is 285. For a 95 wt% resin and 5 wt% diluent mixture the EEW is calculated to be 17.75.

Hardener

A polyfunctional aliphatic amine triethylene tetramine (TETA), $C_6H_{18}N_4$, is used as curing agent. This chemical is commercially known as D.E.H. 24 and manufactured by DOW Chemical Company. Molecular weight of this hardener is 146.4 and weight per active hydrogen is 24.4. Phr (parts per hundred parts of resin) of amine for 95:5% by weight resin–diluent mix is calculated to be 13.74. For the selected combination of epoxy resin and hardener, the curing schedule is to gel at room temp and then post-cure at 100 °C for 3 h.

Microballoons

Three different types of borosilicate glass microballoons are used for the fabrication of syntactic foam specimens in this study. These microballoons are manufactured and supplied by 3 M under the trade name "Scotchlite." Distribution of outer diameter of all types of microballoons is nearly the same, but the internal diameter is different. This causes a difference in the density of different types of microballoons. The physical properties of microballoons such as the mean particle diameter and particle density of the microballoons (as supplied by the manufacturer) are given in Table 1.

Gupta and Woldesenbet [12] have introduced the concept of the radius ratio, η, parameter and the relationship of the radius ratio and microballoon wall thickness is given by Eq. 1.

$$\eta = \frac{r_0 - t}{r_0} = \frac{r_1}{r_0} \tag{1}$$

where t is the wall thickness, r_1 is the internal radius, and r_0 is the outer radius of the microballoon. The radius ratio, η, varies between 0 and 1. The wall thickness decreases correspondingly when η increases leading to a decrease in the density of the microballoon. Similarly, when η decreases, the density of the microballoon increases, and therefore, the syntactic foam's density increases. All selected types of microballoons have η value more than the critical value of 0.71 to make the direct comparison of experimental results meaningful [27]. It was theoretically established that syntactic foams having η value higher than 0.71 experience similar stress states in the specimens during compression testing where the fracture of the microballoons did not induce compression on the matrix.

Mold

Stainless steel molds having inner dimensions of $240 \times 240 \times 13$ mm^3 are used for casting the syntactic foams. No vacuum or pressure is applied during the casting or curing of syntactic foam slabs. Dow Corning 111 Sealant and Lubricant is used as release agent in the molds. This lubricant is silicone-based white translucent gel. Selection of this release agent is based on its service temperature range of -40 to 204 °C and bleed characteristics, 0.5% in 24 h at 200 °C.

Syntactic foam

The fractured surface of typical syntactic foam, SF3260, clearly shows the microballoons and the epoxy matrix is shown in Fig. 1. The volume fractions of the microballoons in the syntactic foams are maintained at 0.1, 0.2, 0.3, 0.4, 0.5, and 0.6. Three types of microballoons, S32, S38, and K46, are used. The microballoons have the same mean outer radius of 40 μm, but different internal radii leading to a difference in their density. This density difference causes the density of syntactic foams to change without changing the volume fractions of microballoons and matrix material in the structure. The same volume fraction provides a constant interfacial area between matrix and microballoons, and variation of properties can be directly related only to the difference in wall thickness. Resin and diluent are mixed together and heated to 50 °C to further reduce the viscosity of the mix for uniform mixing and complete wetting of microballoons. The hardener is then mixed and the microballoons are added to this resin system mixture. The ratio of hardener to matrix resin used is 0.138. This mixture is then cast in molds and allowed to cure. All the fabricated slabs were cured for 36 h at room temperature and then post-cured for 3 h at 100 ± 3 °C. Standard ASTM C 271-94 is used to measure the densities of the fabricated syntactic foams. The results of the density calculation are presented in Table 2.

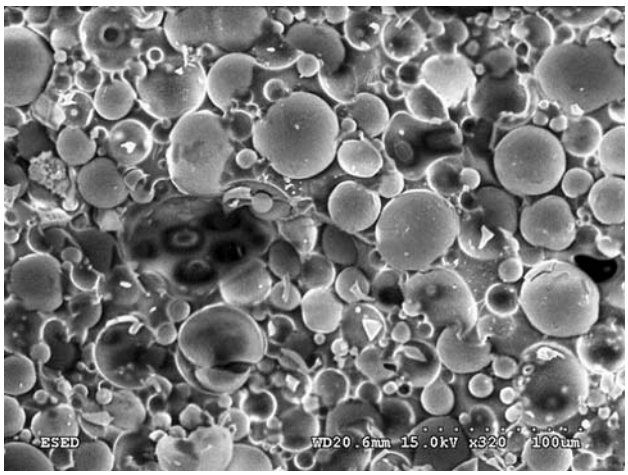

Fig. 1 Structure of SF3260 syntactic foam

Table 1 Properties of microballoons used to fabricate syntactic foams

Microballoon type	Microballoon density (kg/m^3)	Mean microballoon diameter (μm)	Average wall thickness (μm)	Calculated radius ratio η
S32	320	40	1.86	0.907
S38	380	40	2.23	0.888
K46	460	40	2.74	0.863

Table 2 Density of fabricated syntactic foams

Microballoon type	Volume fraction (%)	Corresponding foam nomenclature	Syntactic foam density (kg/m^3)
S32	10	SF3210	1,020
S38		SF3810	1,035
K46		SF4610	1,043
S32	20	SF3220	946
S38		SF3820	966
K46		SF4620	973
S32	30	SF3230	861
S38		SF3830	877
K46		SF4630	902
S32	40	SF3240	760
S38		SF3840	785
K46		SF4640	815
S32	50	SF3250	650
S38		SF3850	682
K46		SF4650	722
S32	60	SF3260	545
S38		SF3860	575
K46		SF4660	685

Compression test parameters

ASTM standards have been followed wherever applicable in this work and have been given preference over any other standards that may exist on similar topics. ASTM D 695-96 was selected for the compression testing of syntactic foams. This standard is for unreinforced and reinforced rigid plastic type of materials. Some other researchers had also followed the same standard according to the earlier published experimental work [10]. Specimen dimensions recommended in ASTM D 695-96 for continuous cores were selected for syntactic foam specimens. The specimen cross section was 25.4×12.5 mm^2 and height was 25.4 mm. For the compression testing, MTS 810 Material Test System with microprocessor-controlled data acquisition system was used. Crosshead movement was maintained at 1.3 mm/min. For each type of syntactic foam at least five specimens were tested. The compressive strength and modulus are calculated using the load and displacement data obtained from the machine. This compression rate corresponds to a strain rate of about 3×10^{-4} s^{-1}.

Split-Hopkinson pressure bar apparatus

A SHPB test setup was designed and built for dynamic type compression testing of various materials for strain rates exceeding several hundreds per second. The principal application of the Hopkinson Pressure Bar has been in the study of the transient response of a material to dynamic loading [28]. It basically consists of a pneumatic loading device, which includes a pressure chamber, gun barrel, and release valve. It also consists of incident and transmitted pressure bars and a striker bar supported by Teflon bearings. The diameter of the bars is 9.5 mm and the lengths of the striker, incident, and transmitted bars are 152, 1,220, and 610 mm, respectively. The material used for striker bar and the pressure bars is a maraging steel having very high values of yield strength (1,830 MPa) to withstand a very high impact velocity. These pressure bars are mounted on a rigid beam. Syntactic foam specimens with an average diameter of 9.3 mm and an aspect ratio of one are sandwiched between the two pressure bars. A frictional constraint exists at the pressure bar–specimen interface due to the radial expansion of the specimen during loading. The frictional effects are the highest when the specimen is at rest and this may produce non-uniform deformation in the specimen. By applying a thin film of lubricant at the interfaces, these frictional constraints have been significantly reduced [29]. Hence, in the present study molybdenum disulfide lubricant is applied.

A photograph of the SHPB apparatus is shown in Fig. 2. The loading pulse in these experiments is initiated by an axial impact on the free end of the input bar by the striker bar, which is accelerated by a long gun barrel. To control the velocity of the striker bar to a desired velocity, the air pressure is controlled by regulators. Strain gauges (with resistance of 350 Ohms and Gauge Factor of 2.10 at room temperature) are mounted on incident and transmitter pressure bars at the distance of 18.5 cm from the junction ends of both pressure bars. The gauges are connected to a signal bridge conditioner. The strain gauge signal is amplified and recorded by digital processing oscilloscope. After an impact caused by the striker bar, an elastic compressive wave of a constant amplitude and a finite duration

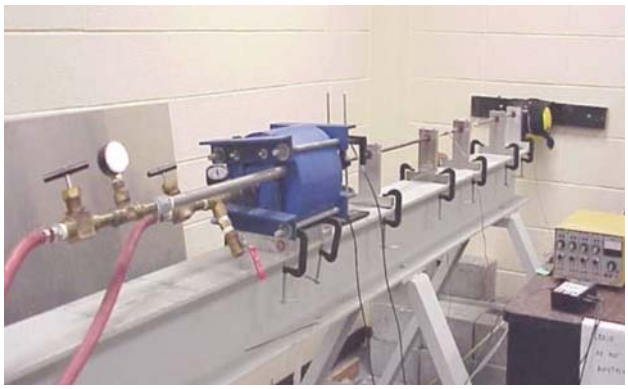

Fig. 2 Split-Hopkinson bar apparatus

is generated in the input pressure bar. The incident pulse wavelength can be adjusted by using striker bars of different lengths, as the pulse in the incident bar is twice the length of the striker bar. The SHPB is also modified with pulse shapers to minimize wave dispersions and obtain the right shape of the wave. The amplitude of the pulse is also directly proportional to the impact velocity of the striker bar [30]. When the compressive loading pulse in the incident pressure bar reaches the specimen, some part of the pulse gets reflected from the specimen–input bar interface, while some part is transmitted to the transmitted bar. The magnitudes of these reflected and transmitted pulses will decide the physical properties of the specimen. The overall specimen dimensions are required to be small enough to minimize the effects of longitudinal and lateral inertia and wave dispersion within the specimen. High numbers of internal reflections are experienced in the short specimen during the duration of the loading pulse since the loading pulse is long compared to the wave transit time in the specimen. The reflections cause the stress distribution in the specimen to be uniform [31].

One-dimensional wave propagation is assumed to be true for analyzing the strain signals from the strain gauges. If the modulus, cross section area, and density of bars are denoted by E_b, A_b, and ρ_b and those for specimen are E_s, A_s, and ρ_s, respectively, the equations for the strain rate ($\dot{\varepsilon}$), strain (ε), and stress (σ) of the specimen are given by [32]:

$$\frac{d\varepsilon(t)}{dt} = \frac{C_o}{L_s}[\varepsilon_I(t) - \varepsilon_R(t) - \varepsilon_T(t)] \quad (2)$$

$$\frac{d\varepsilon(t)}{dt} = \frac{-2C_o}{L_s}\varepsilon_R(t) \quad (3)$$

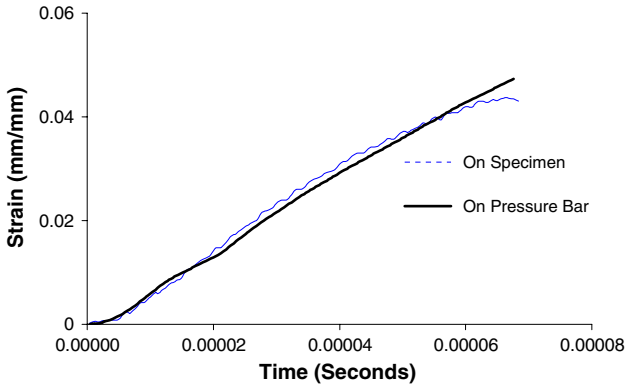

Fig. 3 Comparison of strain values obtained by direct strain measurement and by using SHPB

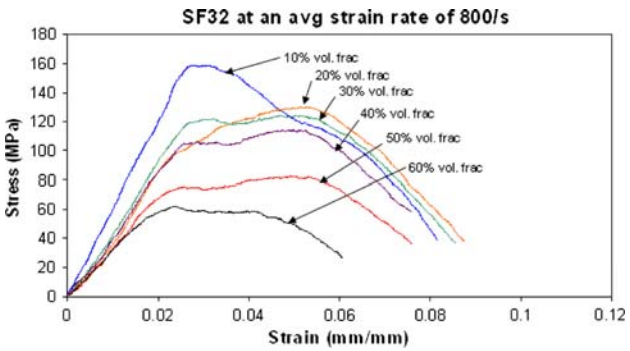

Fig. 4 Stress versus strain curves for 10–60% volume fraction of S32 microballoons obtained at approximately 800 s^{-1} strain rate

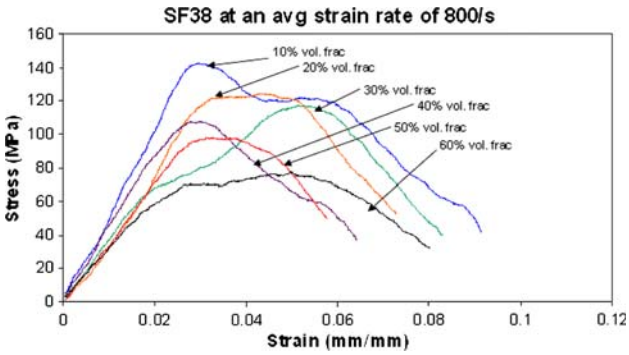

Fig. 5 Stress versus strain curves for 10–60% volume fraction of S38 microballoons obtained at approximately 800 s^{-1} strain rate

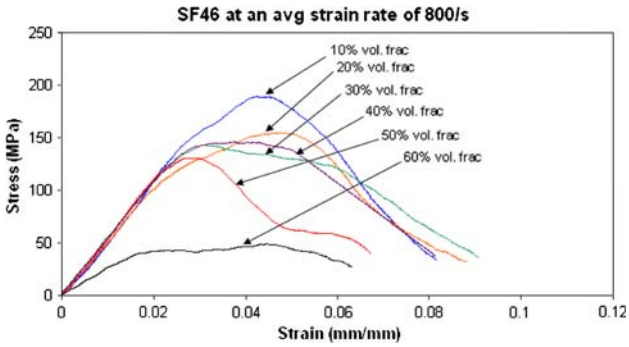

Fig. 6 Stress versus strain curves for 10–60% volume fraction of S32 microballoons obtained at approximately 800 s^{-1} strain rate

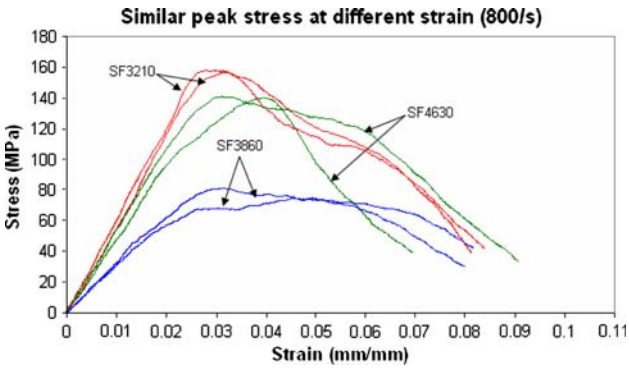

Fig. 7 Varying strains for the same strain rate and same type of syntactic foam

The instantaneous strain value can be calculated by

$$\varepsilon(t) = \frac{-2C_o}{L_s}\int_0^t \varepsilon_R(t)dt \quad (4)$$

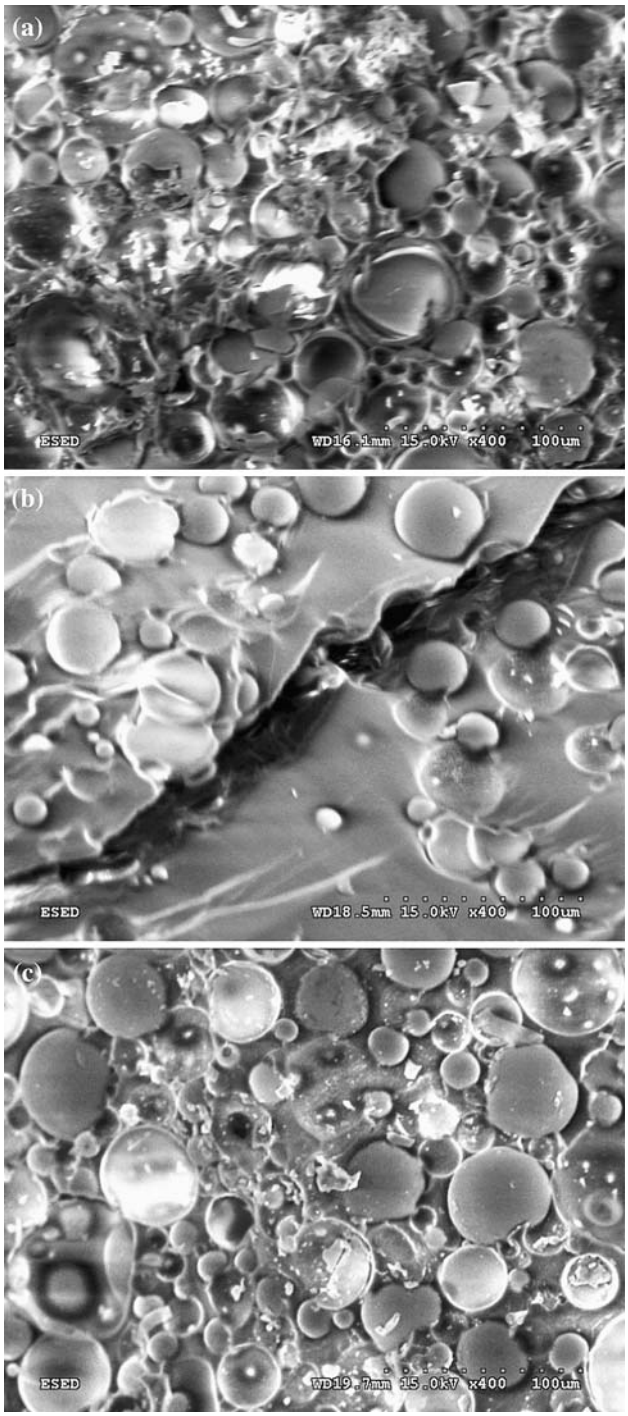

Fig. 8 Scanning electron microscopy (SEM) pictures of fractured surfaces of **a** SF3860 at quasi-static, **b** SF4630 at ~450/s, and **c** SF3260 at ~800/s specimens

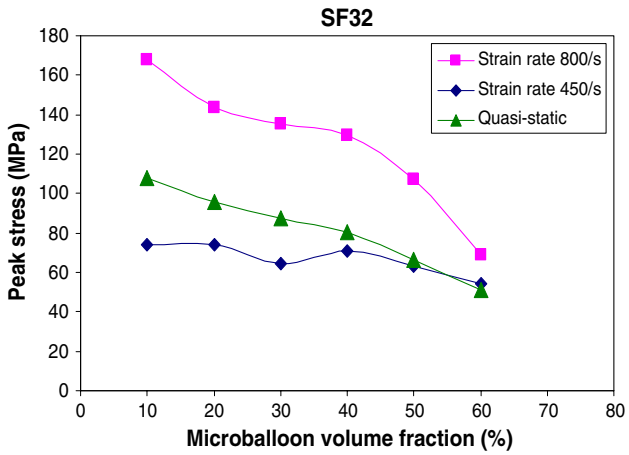

Fig. 9 Maximum stress versus microballoon volume fraction for SF32 syntactic foams at varying strain rates

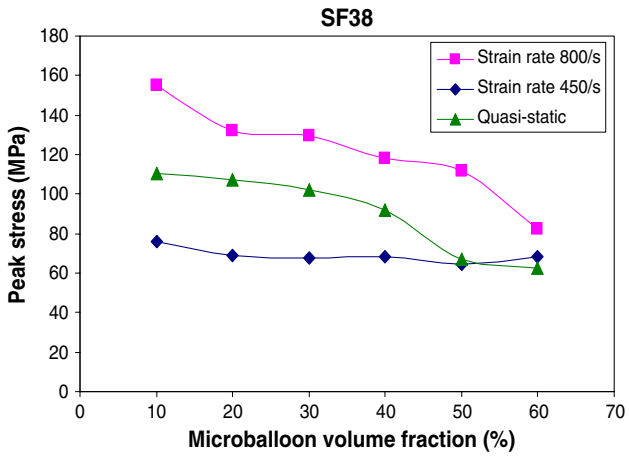

Fig. 10 Maximum stress versus microballoon volume fraction for SF38 syntactic foams at varying strain rates

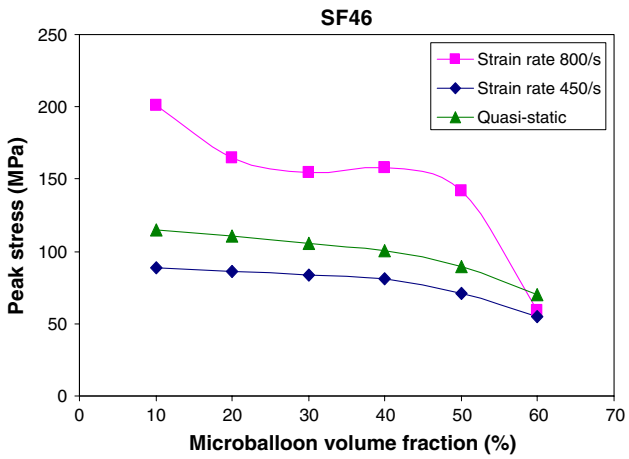

Fig. 11 Maximum stress versus microballoon volume fraction for SF46 syntactic foams at varying strain rates

and the stress by

$$\sigma(t) = \frac{E_b A_b}{A_s}\varepsilon_T(t) \quad (5)$$

$$C_o = \sqrt{E_b/\rho_b} \quad (6)$$

where C_o is the velocity of the bar, L_S is the length of the specimen, and $\varepsilon_I(t)$, $\varepsilon_R(t)$, and $\varepsilon_T(t)$ are the strain gauge signals of the incident, reflected, and transmitted pulses, respectively.

Equations 2–5 are based on the assumption that dynamic forces in both incident and transmitter bars are equal and can be expressed as

$$\varepsilon_I + \varepsilon_R = \varepsilon_T \quad (7)$$

From Eqs. 3–5, it is clear that the strain can be obtained by integrating the reflected pulse and the stress in the specimen from the transmitted pulse. To validate the results obtained from the SHPB strain gauges, a sample specimen was fitted with a strain gauge and tested. The strain results from both measurements were found to be similar (Fig. 3).

Results and discussion

Stress–strain behavior

The volume fraction effect on the high strain rate compression properties of syntactic foams is presented. The dynamic results are compared to the quasi-static results for the same type of syntactic foams to understand the effect of volume fraction at different strain rates. Eighteen types of specimen are tested both at quasi-static and at three different high strain rates. Figures 4, 5, and 6 show the typical stress versus strain curves for the six microballoon volume fraction, 0.1, 0.2, 0.3, 0.4, 0.5, and 0.6, syntactic foams obtained at approximately 800 s^{-1} strain rate and composed of three types of microballoons, S32, S38, and K46. The results show that there is quite a dramatic effect of volume fraction on the high strain rate properties of syntactic foams. Each figure indicates that varying the volume fraction changes the behavior of syntactic foams. The variation of microballoon volume fraction is directly related to the density of the syntactic foam, as shown in

Table 3 Volume fraction effect on the modulus and peak stress values of syntactic foams having S32 microballoons at varying strain rates

Vol. frac (%)	SF32			
	Strain rate (s^{-1})	Modulus (MPa)	Peak stress (MPa)	Maximum strain (mm/mm)
10	578.4	2950 ± 55	74 ± 12	0.03229
	617.38	3631 ± 51	133 ± 13	0.05386
	775.69	4945 ± 60	168 ± 4	0.03512
	Quasi-static	2430.3	107.58	
20	469.97	2851 ± 58	65 ± 6	0.02343
	671.15	3572 ± 21	126 ± 8	0.03497
	847.69	4221 ± 52	131 ± 9	0.05381
	Quasi-static	2334.94	96.03	
30	504.57	2311 ± 31	61 ± 4	0.02152
	676.8	3344 + 29	126 ± 10	0.03692
	794.95	4024 ± 36	155 ± 6	0.0434
	Quasi-static	2281.8	87.49	
40	463.04	2110 ± 63	64 ± 3	0.02265
	567.64	3178 ± 71	106 ± 5	0.03298
	791.99	3774 ± 33	125 ± 9	0.04257
	Quasi-static	2252	80.69	
50	477.77	1967 ± 44	55 ± 7	0.02525
	661.12	2910 ± 31	61 ± 6	0.04017
	863	3550 ± 49	119 ± 12	0.0592
	Quasi-static	2051.6	66.66	
60	474.03	1845 ± 45	42 ± 3	0.02559
	654.12	2657 ± 40	54 ± 3	0.02467
	942.89	3364 ± 77	81 ± 10	0.07732
	Quasi-static	1878.11	50.96	

Table 2. It is evident that as the microballoon volume fraction increases, the density of the syntactic foam decreases, due to the increasing void content. The peak stress values for all types of syntactic foams made of three microballoons of different radius ratios decrease as the microballoon volume fraction increases. The strain values where these peak stresses occur change depending on the volume fraction of the microballoons. However, unlike the peak stress, there is both an increasing and decreasing trend when the volume fraction increases even when the microballoons are the same. The fact that there is no apparent trend in the strain values strongly indicates that the critical strain at which peak strength is observed does not depend on the type of microballoons and can be primarily recognized as the matrix property as similarly concluded by Woldesenbet et al. previously [23]. Another explanation to this behavior is that the microstructure arrangement of the microballoons in the matrix material is random as shown in Fig. 1. Therefore, it is expected that the strain, which is dependent on the deformation, relies on the microballoons and matrix distribution. This distribution is random and affects the fracture modes even for samples of the same volume fraction creating no specific trend. This argument is confirmed by looking at the strain values at peak stress for the same type of syntactic foam tested at the same strain rate as shown in Fig. 7. Figure 7 shows three pairs of graphs of the same syntactic foam tested at high strain rate. Pairs of SF32 at 10%, SF38 at 60%, and SF46 at 30% graphs clearly demonstrate that the peak stresses are similar for each pair while the strains at the peak stresses are different.

Strain energy

Figures 4, 5, and 6 also demonstrate the effect of volume fraction on the total strain energy absorbed at high strain rate. It is found that the total strain energy is indirectly related to the volume fraction. Therefore, in all three types of syntactic foams made of different types of microballoons, the strain energy absorbed decreases as the volume fraction increases. The strain energy decreases up to 80% as the microballoon volume fraction increases from 10 to 60%. This decrease in the total strain energy can be understood by looking at the energy absorbed as equivalent

Table 4 Volume fraction effect on the modulus and peak stress values of syntactic foams having S38 microballoons at varying strain rates

Vol. frac (%)	SF38			
	Strain rate (s^{-1})	Modulus (MPa)	Peak stress (MPa)	Maximum strain (mm/mm)
10	495.73	3121 ± 33	76 ± 5	0.024066
	591.13	4046 ± 63	145 ± 4	0.0378
	742.97	5239 ± 66	184 ± 17	0.03599
	Quasi-static	2551.39	110.71	
20	484.94	3048 ± 21	66 ± 3	0.01958
	561.62	3839 ± 31	128 ± 5	0.02564
	774.36	4803 ± 44	132 ± 4	0.03835
	Quasi-static	2228.88	107.42	
30	512.74	2619 ± 39	68 ± 7	0.02714
	651.01	3883 ± 60	129 ± 10	0.03453
	830.82	4454 ± 29	158 ± 9	0.02904
	Quasi-static	2325.66	102.2	
40	475.39	2593 ± 40	68 ± 4	0.024335
	591.12	3493 ± 44	111 ± 9	0.03177
	787.09	3984 + 50	144 ± 56	0.03561
	Quasi-static	2350.66	91.67	
50	445.09	2240 ± 33	58 ± 4	0.02692
	670.06	3133 ± 70	65 ± 7	0.03874
	923.35	4389.2 ± 52	129 ± 4	0.07349
	Quasi-static	2086.66	66.82	
60	480.57	2259 ± 60	55 ± 4	0.02529
	647.34	2744 ± 24	58 ± 6	0.05257
	954.55	3881 ± 47	130 ± 15	0.07992
	Quasi-static	2099.33	62.62	

to the amount of energy required for crack propagation. As the microballoon volume fraction increases, the energy required for crack propagation decreases because of the additional interfaces introduced in the matrix material when more microballoons are added. These additional interfaces provide preferential propagation paths and create fractured surfaces easily at lower energy levels. The strain energy as expected shows dependence on the strain rate as calculated from the areas under the stress versus strain graphs at the different strain rates used in the experiments. The strain energy increases as the strain rate increases for the same syntactic foam having the same microballoons. The reason is that as the strain rate increases, the crack propagates fast and forms vertical splitting of the specimen. The vertical crack fractures the microballoons or cuts through the matrix indiscriminately rather than choosing a preferential path of least resistance. This occurs more as the strain rate increases. Figure 8 shows several fractured surfaces at varying strain rates illustrating the strain rate effect on strain energy.

Strain rate effect

The stress versus strain graphs and strain energy discussed provide a general overview of the effect of microballoons volume fraction at high strain rates. However, it is critical to understand the magnitude of this volume fraction effect at different strain rates including quasi-static strain rates. Figures 9, 10, and 11 show the maximum stress versus volume fraction for SF32, SF38, and SF46 syntactic foams at varying strain rates, respectively. The results, including standard deviation, are also given in Tables 3, 4, and 5. From Figs. 9, 10, and 11, the peak stress values are observed to significantly vary when the strain rate changes. It is quite unexpected that the peak stress values at quasi-static are higher than the values at around 450/s. In SF32 and SF38, with microballoon's wall thickness less than SF46's, the quasi-static peak stresses are higher for volume fractions in the range of 10–40%, but similar for 50 and 60%. For SF46, the quasi-static peak stress values are higher for all volume fractions. This phenomenon is caused by change in the mode of fracture and is demonstrated with the help of micrographs of fractured surfaces. Figure 12 shows the SEM images of fractured surfaces of SF4630 tested at quasi-static and 441/s strain rates. Figure 12a, corresponding to quasi-static loading fracture surface of SF4630 specimen, exhibits crushing of the microballoons and matrix shearing. The crushing of the microballoons creates high stress values in quasi-static testing for syntactic foams because of the increased load requirement to break the glass microballoons. Comparing the values at quasi-static and 450/s strain rates from Figs. 9, 10, and 11, it can be inferred that the increase of the peak stress of the syntactic foam at quasi-static loading is found to be higher than the increase of peak stress due to high strain rate effect on the matrix. The matrix is proven to be more strain rate sensitive than the microballoons or the reinforcing component [23, 33, 34]. Figure 12b, corresponding to the fracture surface of the specimen tested at 450/s strain rate, indicates that the crack propagates through either the matrix material or the matrix-microballoon interfaces.

For SF32 and SF38 at 50 and 60% volume fraction where the quasi-static and 450/s peak stress values are similar, the mode of fracture is dominated by microballoon fracture as shown in Figs. 13 and 14. At these microballoon volume fractions, the matrix role is reduced greatly, and the crushing of the microballoons at quasi-static and the fracture of microballoons at approximately 450/s strain rate demonstrate similar effect. For SF46, the crushing of thicker wall microballoons requires more force at quasi-static than at 450/s strain rate where there is limited rupture of microballoons, and therefore the peak stress at quasi-static is higher than at 450/s strain state at all volume

Table 5 Volume fraction effect on the modulus and peak stress values of syntactic foams having K46 microballoons at varying strain rates

Vol. frac (%)	SF46			
	Strain rate	Modulus	Peak stress	Maximum strain
10	454.23	3503 ± 39	78 ± 5	0.0219
	519.56	4545 ± 69	148 ± 3	0.0265
	601.34	6062 ± 45	190 ± 10	0.0303
	Quasi-static	3719.304	113.41	
20	403.64	3130 ± 32	73 ± 2	0.020339
	540.97	42324 ± 44	138 ± 6	0.02448
	600.82	5412 ± 23	164 ± 3	0.02926
	Quasi-static	2670	110.25	
30	441.54	2856 ± 57	71 ± 2	0.0242
	605.03	4552 ± 31	132 ± 9	0.0318
	694.37	4859 ± 25	161 ± 5	0.0519
	Quasi-static	2508	105.19	
40	450.01	2713 ± 81	81 ± 3	0.02169
	665.68	3973 ± 52	129 ± 6	0.02154
	756.33	4395 ± 27	158 ± 4	0.03748
	Quasi-static	2414.13	100.816	
50	490.54	2460 ± 47	64 ± 7	0.02463
	635.92	3217 ± 37	71 ± 5	0.02378
	798.5	4630 ± 11	139 ± 12	0.05905
	Quasi-static	2473	89.51	
60	483.52	2378 ± 21	55 ± 6	0.026
	624.67	3000 ± 33	59 ± 2	0.0462
	722.56	4335 ± 54	130 ± 15	0.0707
	Quasi-static	2259.66	64.158	

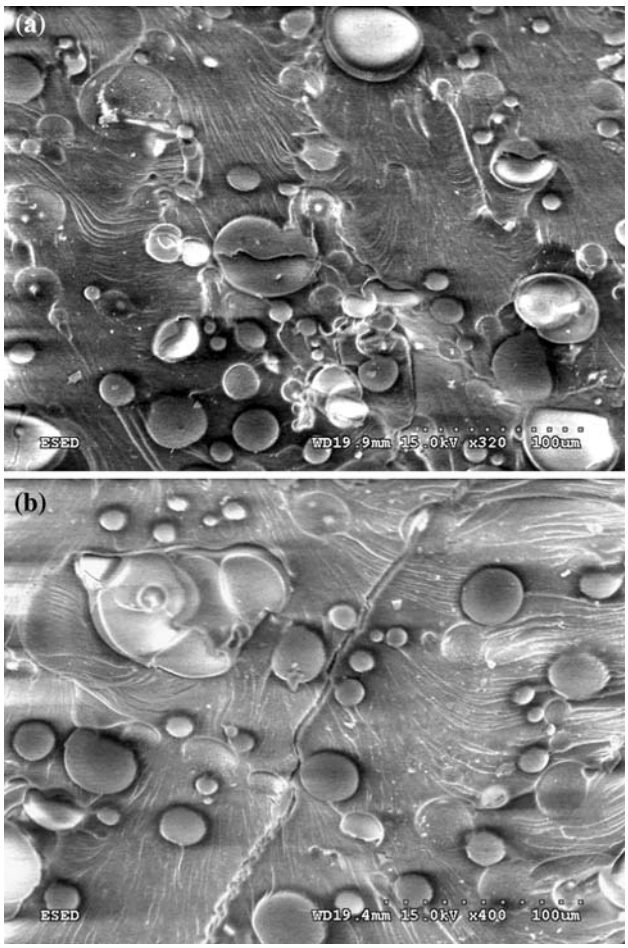

Fig. 12 SEM images of fractured surfaces of SF4630 tested at **a** quasi-static and **b** 441/s strain rates

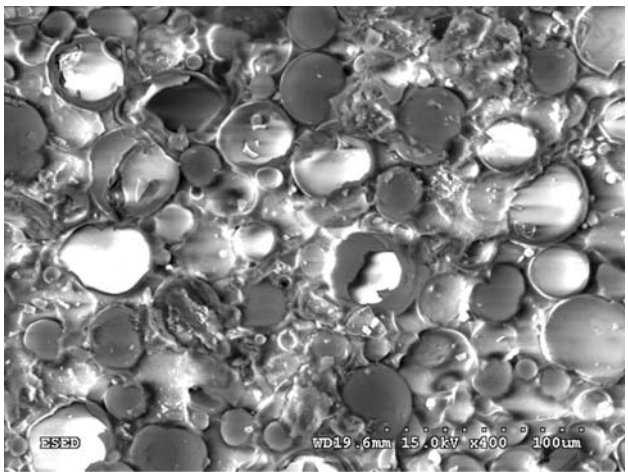

Fig. 13 SEM image of a fractured surface of SF3260 tested at 470/s strain rate

fractions, as shown in Fig. 11. For the case of higher strain rates, such as 800/s, the peak stress values are significantly higher for all types of syntactic foam and volume fractions

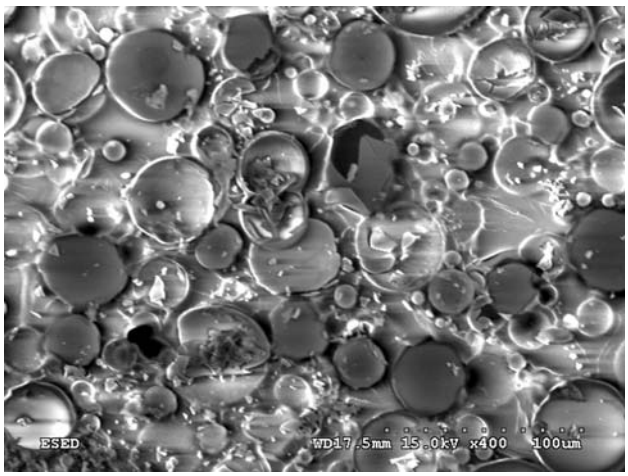

Fig. 14 SEM image of a fractured surface of SF3850 tested at 440/s strain rate

except SF46 at 60% volume fraction. The high peak stress values indicate the high force requirement to fracture the microballoons for the different syntactic foams and volume fractions, and the matrix sensitivity of strain rate. SEM image of SF4630 showing clear fracture of microballoons is shown in Fig. 15. For SF4660, the K46 microballoons have the thickest wall and SF4660 has the highest volume fraction. Therefore, the crushing force required at quasi-static is equivalent to the force required to fracture the microballoons at the higher strain rates of 450 and 800/s, and this leads to the similarity of SF4660 peak stresses at all strain rates.

The strain rate effect on the dynamic modulus is dominant at lower volume fraction for all types of syntactic foams. Figures 16, 17, and 18 demonstrate this effect for SF32, SF38, and SF46 at volume fractions ranging from 10 to 60%. The strain rate effect variation is due to the matrix strain rate sensitivity [23, 33, 34]. As the microballoon volume fraction increases above 20%, the effect of strain rate on the modulus decreases. This is indicated by similar differences in the modulus values at different volume fractions in Figs. 16 17, and 18, except a few cases discussed below. For SF32, the effect of strain rate on the modulus remains the same after 20% except the differences between the quasi-static and 450/s modulus in the 40–60% range. Actually, the modulus difference approaches zero at 60%. This indicates that matrix influence is minimized and the fracture mode for both quasi-static and 450/s strain rate is similar, that is, microballoon fracture. Similar explanation is attributed to the behavior of SF38 after 40% volume fraction. For SF46, 50 and 60% show reduced strain rate dependency. In particular, SF4660 at 800/s has the same modulus as quasi-static and 450/s. This result is the manifestation of not only the effect of volume fraction but also that of the wall thickness or radius ratio of the

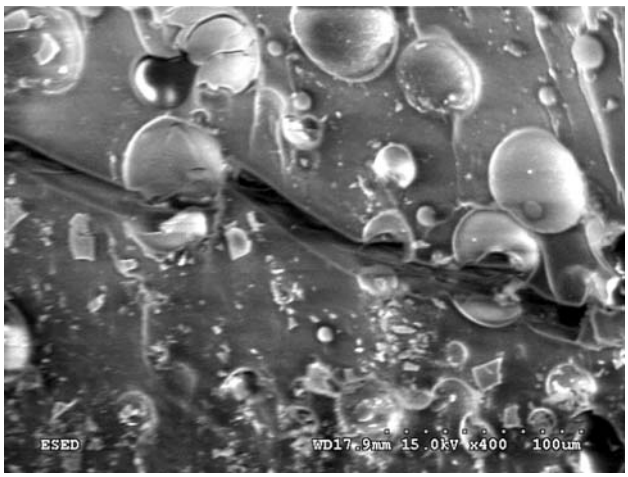

Fig. 15 SEM image of a fractured surface of SF4630 tested at high strain rate

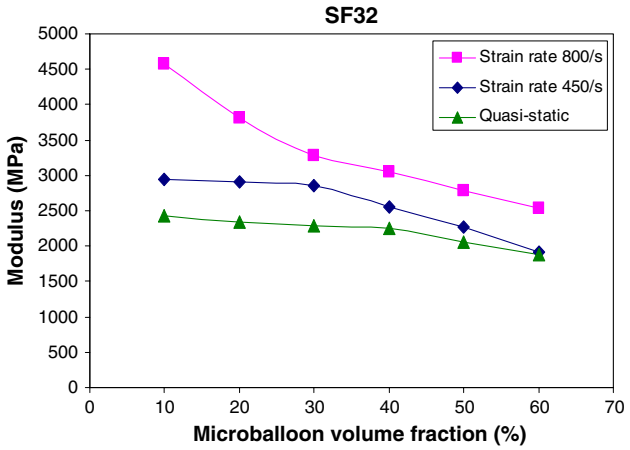

Fig. 16 Modulus versus microballoon volume fraction for SF32 syntactic foams at varying strain rates

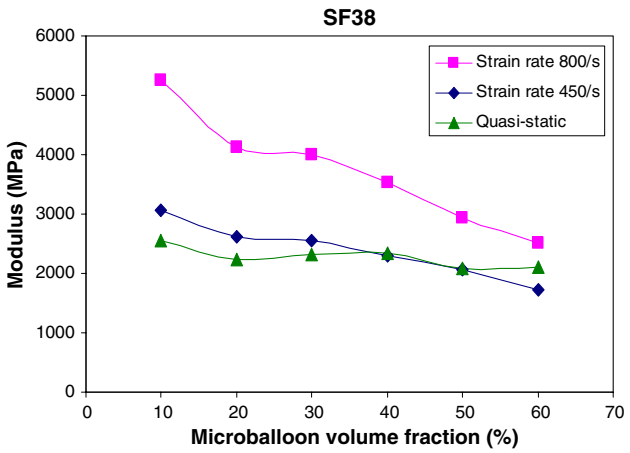

Fig. 17 Modulus versus microballoon volume fraction for SF38 syntactic foams at varying strain rates

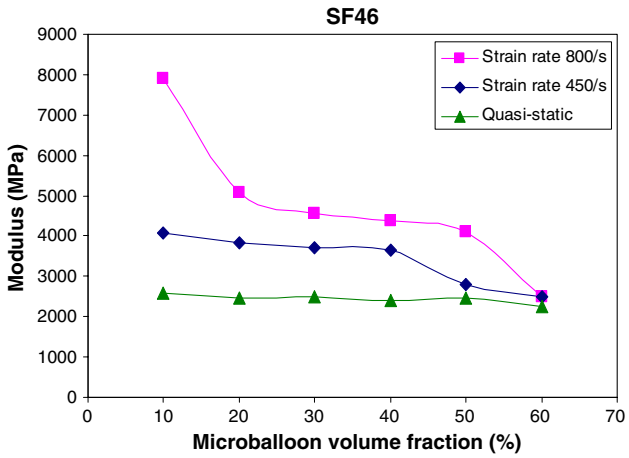

Fig. 18 Modulus versus microballoon volume fraction for SF32 syntactic foams at varying strain rates

microballoons on the high strain rate behavior of syntactic foam [35]. Similar stiffness for all SF4660 tests carried out at three different strain rates is an indication that rupture of microballoons is the dominant mode of fracture, and the microballoons play the major role in the determination of the stiffness due to the increased wall thickness.

Conclusion

Microballoon volume fraction effect on the high strain rate compressive properties of syntactic foams is studied using six volume fractions and three different types of microballoons. The high strain rate behavior of syntactic foams is found to be affected by the volume fraction. The peak stress values for all types of syntactic foams decrease as the microballoon volume fraction increases. The strain values where these peak stresses occur change depending on the volume fraction of the microballoons. Even though particular syntactic foam is composed of the same microballoon, unlike the peak stress, there is both an increasing and decreasing trend in strain values when the volume fraction increases.

The peak stress values at quasi-static are in general higher than the values at around 450/s in these syntactic foams. This trend is caused by change in the mode of fracture and is demonstrated with the help of SEM micrographs of fractured surfaces. The SEM indicates significant amount of crushing in quasi-static tested specimen creating high stress. The SEM also points out that the crack propagates through either the matrix material or the matrix-microballoon interfaces in the 450/s tested specimen causing reduced stress. The strain rate effect on the dynamic modulus is found to be dominant at lower volume fraction for all types of syntactic foams. This research

demonstrates that the matrix influence is minimized on the high strain rate behavior of syntactic foam when the volume fraction increases. Instead the fracture mode is established to play a major role in determining the stress and modulus values at high volume fraction. The syntactic foam at 60% volume fraction is found to be more strain rate independent.

Acknowledgements This work was supported by DOW Chemical Company, 3M, and National Science Foundation (Grant No. HRD-0734845).

References

1. Gibson LJ, Ashby MF (1997) Cellular solids, structures and properties. Cambridge, UK
2. Ashida K (1995) Handbook of plastic foams: types, properties, manufacture and applications. New Jersey
3. Karthikeyan CS, Kishor, Sankaran S (2001) J Reinf Plast Comp 20(11):982
4. Gupta N, Woldesenbet E (2003) Compos Struct 61:311
5. Shutov FV (1986) Adv Polym Sci 73:63
6. Kim HH, Oh HH (2000) J Appl Polym Sci 76:1324
7. Smiley LH (1986) Mater Eng 103:27
8. Noor AK, Burton WS, Bert CW (1996) Appl Mech Rev 49:155
9. Gupta N, Kishore, Woldesenbet E, Sankaran S (2001) J Mater Sci 36:4485. doi:10.1023/A:1017986820603
10. Corigliano A, Rizzi E, Papa E (2000) Compos Sci Technol 60:2169
11. Narkis M, Puterman M, Kenig S (1980) J Cell Plast 16:326
12. Gupta N, Woldesenbet E (2004) J Cell Plast 40:461
13. Karthikeyan CS, Sankaran S, Jagdish Kumar MN et al (2001) J Appl Poly Sci 81:405
14. Rizzi E, Papa E, Corignlina A (2000) Int J Solids Struct 37:5773
15. Bunn R, Mottram JT (1993) Composites 24(7):565
16. Progelhof RC. In Proceedings of Instrumented Impact Testing of Plastics and Composite Materials, Houston, March (ASTM), p 105
17. Sounik DF, Gansen P, Clemons JL et al (1997) J Mater Manuf 106(5):211
18. Chen W, Lu F, Winfree N (2002) Exp Mech 42(1):62
19. Rinde A, Hoge KG (1971) J Appl Polym Sci 15:1377
20. Baker WE, Togami TC, Weider JC (1998) Int J Impact Eng 21(3):149
21. Zhao H, Gary G (1998) Int J Impact Eng 21(10):827
22. Song B, Chen W, Frew DJ (2004) J Compos Mater 38:915
23. Woldesenbet E, Gupta N, Jadhav A (2005) J Mater Sci 40:4009. doi:10.1007/s10853-005-1910-2
24. Cohen A, Yalvac S, Wetters DG (1992) In: 37th International SAMPE Symposium and Exhibition, Anaheim, CA, March 1992, (SAMPE), p 641
25. Hiel C, Dittman D, Ishai O (1993) Composites 24:447
26. Ishai O, Hiel CJ (1992) J Compos Technol Res 14:155
27. Gupta N, Woldesenbet E, Kishore (2002) J Mater Sci 37:3199. doi:10.1023/A:1016166529841
28. Kolsky H (1949) Proc Phys Soc B62:676
29. Kaiser MA, Wicks A, Wilson et al (1998) Thesis Virginia Polytechnic Institute and State University, Blacksburg, Virginia, p 1
30. Gama BA, Gillespie JW, Hassan M et al (2001) J Compos Mater 35:1201
31. Lindholm US (1964) J Mech Phys Solids 12:317
32. Gilat A, Goldberg RK, Roberts GD (2002) Compos Sci Technol 62:1469
33. Woldesenbet E, Vinson JR (1999) AIAA J 37:1102
34. Woldesenbet E, Vinson JR (2001) J Compos Mater 35:509
35. Woldesenbet E, Peters S (2007) In: the Proceedings of the 22nd American Society for Composites Conference, Seattle, Washington